Journal of Hazardous Materials 211–212 (2012) 366–372

Contents lists available at SciVerse ScienceDirect

Journal of Hazardous Materials

journal homepage: www.elsevier.com/locate/jhazmat

Effective removal of heavy metal ions Cd^{2+}, Zn^{2+}, Pb^{2+}, Cu^{2+} from aqueous solution by polymer-modified magnetic nanoparticles

Fei Ge, Meng-Meng Li, Hui Ye, Bao-Xiang Zhao*

Institute of Organic Chemistry, School of Chemistry and Chemical Engineering, Shandong University, Jinan 250100, PR China

ARTICLE INFO

Article history:
Received 3 June 2011
Received in revised form
17 November 2011
Accepted 4 December 2011
Available online 13 December 2011

Keywords:
Magnetic nanoparticles
Polymer
Adsorption
Heavy metal ions

ABSTRACT

We prepared novel Fe_3O_4 magnetic nanoparticles (MNPs) modified with 3-aminopropyltriethoxysilane (APS) and copolymers of acrylic acid (AA) and crotonic acid (CA). The MNPs were characterized by transmission electron microscopy, X-ray diffraction, infra-red spectra and thermogravimetric analysis. We explored the ability of the MNPs for removing heavy metal ions (Cd^{2+}, Zn^{2+}, Pb^{2+} and Cu^{2+}) from aqueous solution. We investigated the adsorption capacity of Fe_3O_4@APS@AA-co-CA at different pH in solution and metal ion uptake capacity as a function of contact time and metal ion concentration. Moreover, adsorption isotherms, kinetics and thermodynamics were studied to understand the mechanism of the synthesized MNPs adsorbing metal ions. In addition, we evaluated the effect of background electrolytes on the adsorption. Furthermore, we explored desorption and reuse of MNPs. Fe_3O_4@APS@AA-co-CA MNPs are excellent for removal of heavy metal ions such as Cd^{2+}, Zn^{2+}, Pb^{2+} and Cu^{2+} from aqueous solution. Furthermore, the MNPs could efficiently remove the metal ions with high maximum adsorption capacity at pH 5.5 and could be used as a reusable adsorbent with convenient conditions.

1. Introduction

Heavy metals released into the environment from plating plants, mining, metal finishing, welding and alloy manufacturing pose a significant threat to the environment and public health. The major concern with heavy metals is their ability to accumulate in the environment and cause heavy metal poisoning. Unlike some organic pollutants, heavy metals are not biodegradable and cannot be metabolized or decomposed. Heavy metals can easily enter the food chain through a number of pathways and cause progressive toxic effects with gradual accumulation in living organisms over their life span. Although acute heavy metal toxicity is rare, chronic low-grade toxicity may be more damaging in the long-term and result in chronic illness. Therefore, reliable methods are needed to remove and detect heavy metals in environmental and biological samples.

A great deal of effort has been devoted to the effective removal of heavy metal ions. The traditional methods commonly used for removal from aqueous solution include ion-exchange [1], solvent extraction [2,3], chemical precipitation [4], nano-filtration [5], reverse osmosis [6] and adsorption [7–10]. The adsorption process is arguably one of the most popular methods for removal and has attracted considerable attention because of its simplicity, convenience and efficiency. Recently, many research groups have explored several nanoparticles for removal because of the ease of modifying their surface functionality and their high surface area-to-volume ratio for increased adsorption capacity and efficiency. In the last decade, magnetic nanoparticle (MNP) adsorption has attracted much interest and is an effective and widely used process because of its simplicity and easy operation [8,11–15].

In recent years, much attention has focused on surface functionalized MNPs such as MNP polymers with core–shell nanostructures, because the polymer shell prevents the core part from particle–particle aggregation and improves the dispersion stability of the core–shell nanostructures in suspension medium [16–23]. Deposition of mesoporous silica layers on MNPs is considered promising for developing magnetic materials for removal of environmental pollutants [24]. Organosilanes are non-poisonous agents widely used in the chemical industry. However, a search of the literature revealed few reports concerning Fe_3O_4@Organosilane@Polymer core–shell–shell magnetic nanostructures for removal of environmental pollutants [25].

Considering the biocompatibility and low toxicity of organosilanes and high adsorption ability of polymers, here we report on our preparation and characterization of novel Fe_3O_4 MNPs modified with 3-aminopropyltriethoxysilane (APS) and copolymers of acrylic acid (AA) and crotonic acid (CA). We investigated the adsorption capacity of Fe_3O_4@APS@AA-co-CA for heavy metal ions Cd^{2+}, Zn^{2+}, Pb^{2+}, Cu^{2+} in different pH solution and metal ion uptake capacity as a function of contact time and metal ion concentration.

* Corresponding author. Tel.: +86 531 88366425; fax: +86 531 88564464.
E-mail addresses: bxzhao@sdu.edu.cn, sduzhao@hotmail.com (B.-X. Zhao).

0304-3894/$ – see front matter © 2011 Elsevier B.V. All rights reserved.
doi:10.1016/j.jhazmat.2011.12.013

We also studied the adsorption isotherms, kinetics and thermodynamics to understand the mechanism of the synthesized MNPs adsorbing metal ions and explored the effect of the background electrolytes, desorption and MNP reuse.

2. Experimental

2.1. Instrumentation

We used a PHS-3C pH-meter (Shanghai, Tianyou) for pH measurement. The concentrations of the metal ions in the solution were measured by use of a flame atomic absorption instrument (Hewlett-Packard 3510). Transmission electron microscopy (TEM) involved use of a JEM-1011 transmission electron microscope. X-ray diffraction (XRD) measurement involved use of a Bruker D8 Advance X-ray diffraction analyzer (Germany) with Copper K-alpha (Cu Kα) radiation. The operation voltage and current were kept at 40 kV and 100 mA, respectively. Infra-red (IR) spectra were recorded with use of an IR spectrophotometer Bruker VERTEX 70 FT-IR (Germany). Thermogravimetric analysis (TGA) involved use of an SDTQ600 thermogravimetric analyzer (USA) at a heating rate of 10 °C/min under a flow of nitrogen. The magnetic property of MNPs was studied by use of a 2900 superconducting quantum interference device (USA). Zeta-potential was measured by ZetaPALS (USA).

2.2. Chemicals and reagents

All chemicals and reagents were analytical grade. Ferric chloride ($FeCl_3{\cdot}6H_2O$), ferrous chloride ($FeCl_2{\cdot}7H_2O$), crotonic acid, tetrahydrofuran (THF), copper chloride ($CuCl_2{\cdot}2H_2O$), cadmium chloride ($CdCl_2{\cdot}2.5H_2O$), zinc chloride ($ZnCl_2$) and lead nitrate ($Pb(NO_3)_2$) were from Sinopharm Chemical. 3-Aminoproyltriethoxysilane (APS) was from J&K chemical. Dicyclohexylcarbodiimide (DCC) was from Aldrich.

2.3. Preparation of magnetic adsorbents

Fe_3O_4 MNPs were prepared by chemical coprecipitation methods [26]. APS-modified Fe_3O_4 (Fe_3O_4@APS) MNPs were synthesized as described [25,27] with some modifications. Briefly, 1.000 g Fe_3O_4 MNPs were dispersed in 120 ml distilled toluene by ultrasonator for 5 min. The dispersion was heated to reflux with mechanical agitation under nitrogen, and then 8 ml APS was added. The mixture underwent refluxing for 3.5 h. The Fe_3O_4@APS MNPs were separated by powerful magnets, then washed with 150 ml anhydrous ethanol 3 times and dried at 60 °C under vacuum for 3 h.

Acrylic acid and crotonic acid copolymer (AA-co-CA) was prepared by free-radical polymerization in distilled toluene as described [28]. In a typical synthesis, crotonic acid (6.000 g), acrylic acid (4.000 g) and distilled toluene (50 ml) were added to a flask with mechanical agitation under nitrogen. The mixture was heated to 70 °C for 10 min. A total of 0.050 g AIBN as an initiator was added. The reaction mixture was kept at 70 °C for 4.5 h. AA-co-CA was precipitated after cooling and filtered under reduced pressure, then washed with 20 ml distilled toluene and dried at 80 °C under vacuum.

AA-co-CA was immoblized on Fe_3O_4@APS by reacting 0.100 g Fe_3O_4@APS with 0.200 g AA-co-CA with catalysis of 0.200 g DCC. The mixture was dispersed in 20 ml distilled THF under ultrasonator for 5 min [29] at room temperature with mechanical agitation for 3.5 h. The product (Fe_3O_4@APS@AA-co-CA) was separated by magnetic fields and washed with 150 ml anhydrous ethanol 3 times, then dried under vacuum at 60 °C.

2.4. Adsorption measurement

Adsorption of metal ions from aqueous solution was measured in batch experiments. We studied the effect of pH (1.0–8.0), kinetics time (0–90 min), and adsorption isotherms (initial concentration 20–450 mg L^{-1}) of metal ions (Cd^{2+}, Zn^{2+}, Pb^{2+} and Cu^{2+}). We also investigated thermodynamics (298–323 K), the effects of alkaline/earth metal ion concentrations (0–0.3 mol L^{-1}), and adsorption isotherms of the naked Fe_3O_4 and Fe_3O_4@APS MNPs to Cu^{2+}. Analyzing adsorption behavior of the MNPs involved adding 0.050 g Fe_3O_4@APS@AA-co-CA to 50 ml of solution of the metal ions at different concentrations at 298 K. The pH was maintained at a constant value during adsorption. The equilibrium time was 45 min, when the adsorption behavior reached equilibrium. The adsorbents were separated by powerful magnets.

2.5. Desorption experiment

To evaluate the ability to reuse the Fe_3O_4@APS@AA-co-CA MNPs, we investigated the effects of concentrations of hydrochloric acid (0–2 mol L^{-1}) on the stability of the adsorbents and the adsorption of metal ions. The desorption experiments involved adding 0.050 g metal ion-loaded adsorbents to 50 ml aqueous solution with 0.1 mol L^{-1} hydrochloric acid. The mixture was shaken for 3 h to reach desorption equilibrium.

3. Results and discussion

3.1. Characterization of the adsorbents

TEM revealed the diameters of the MNPs as typically 15–20 nm (Fig. 1), for a generally homogeneous size. The edges show the immobilization of the copolymers (Fig. 1c).

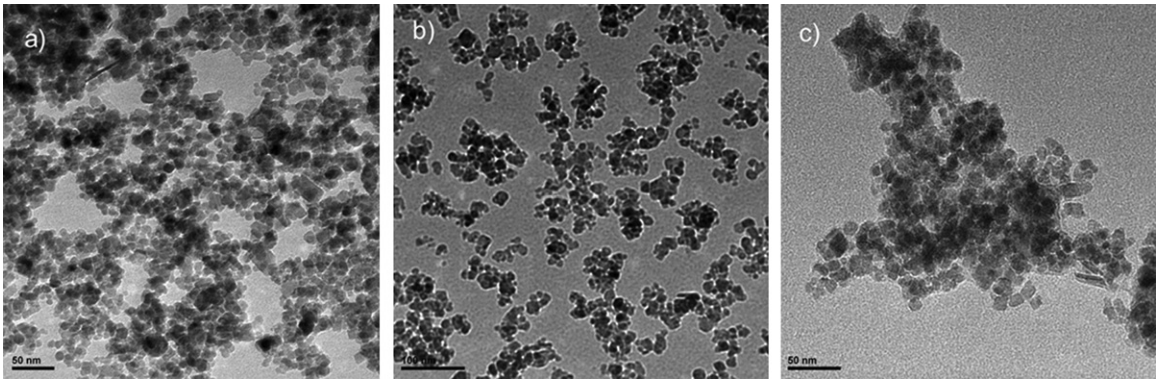

Fig. 1. Transmission electron microscopy of magnetic nanoparticles. (a) Fe_3O_4, (b) Fe_3O_4@APS, and (c) Fe_3O_4@APS@AA-co-CA.

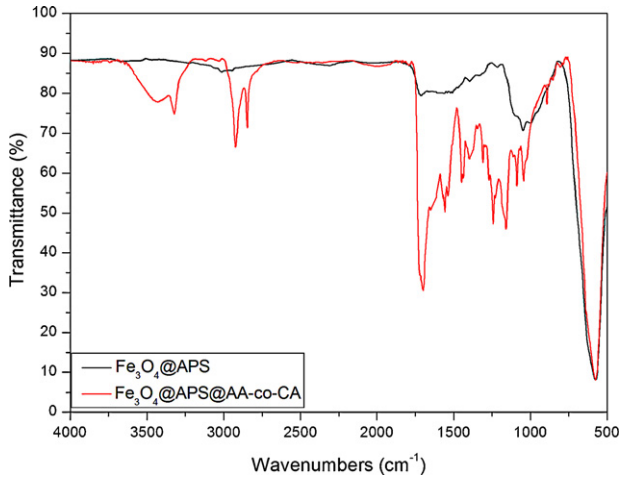

Fig. 2. Fourier transform-infrared analysis of Fe_3O_4@APS and Fe_3O_4@APS@AA-co-CA.

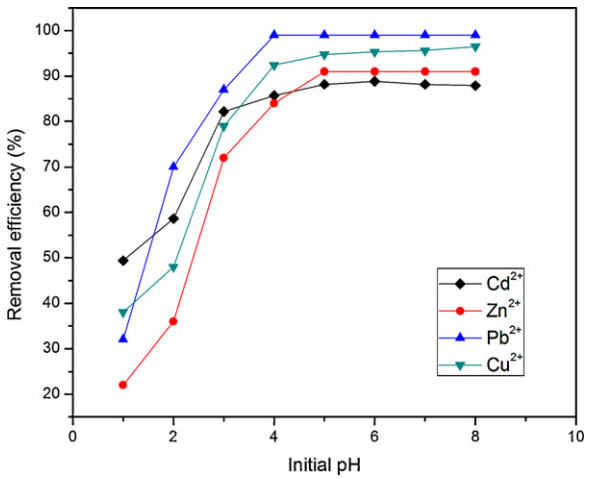

Fig. 4. Effect of pH on the adsorption of metal ions; adsorbent: 0.05 g, concentration of initial metal ions: 100 mg L^{-1}, volume of metal ions solution: 50 ml, time: 2 h, at 298 K.

The 3 types of MNPs possessed superparamagnetic properties, which could be seen from the room-temperature magnetization curves (Supplementary Fig. S1). The saturation magnetization of the naked Fe_3O_4, Fe_3O_4@APS and Fe_3O_4@APS@AA-co-CA MNPs was 79, 67 and 52 emu/g, respectively. The significant reduction in saturation magnetization was due to the amount of nonmagnetic APS and AA-co-CA encapsulated on the Fe_3O_4 MNPs [30].

The surface modification of the Fe_3O_4 MNPs was confirmed by FT-IR. As shown in Fig. 2, peaks of 500–750 cm^{-1} belong to the Fe_3O_4. The introduction of APS to the surface of MNPs was confirmed by bands at 1113 and 1036 cm^{-1} assigned to the Si—O groups. Two broad bands at 3430 and 1620 cm^{-1} were ascribed to the N—H stretching vibration and NH_2 bending mode of free NH_2 groups, respectively. The presence of the anchored ethyl group was confirmed by C—H stretching vibration at 2927 cm^{-1}. The FT-IR spectra for Fe_3O_4@APS@AA-co-CA MNPs showed a broad band at 3326 cm^{-1} attributed to the —OH dimer stretch band. The spectra also showed a strong band around 2927 and 2850 cm^{-1} corresponding to the CH_2 stretching vibrations. The carbonyl group was clearly observed at 1704 cm^{-1}. No strong absorption band appeared at about 1630 cm^{-1}, the characteristic band for C=C stretching vibration of the AA and CA monomers [25,31].

Fig. 3 shows the weight loss with the 3 types of MNPs by TGA curves. The 2 times of weight losses were attributed to the loss of the APS layer and the AA-co-CA layer. The weight increase above 900 °C was caused by the oxidation of Fe_3O_4. From the percentage weight loss in the TGA curves, the weight proportion of the APS and AA-co-CA was estimated at about 4.8% and 36.7%, respectively. Because more copolymers could be grafted onto the surface of APS-modified Fe_3O_4, potential adsorption was expected.

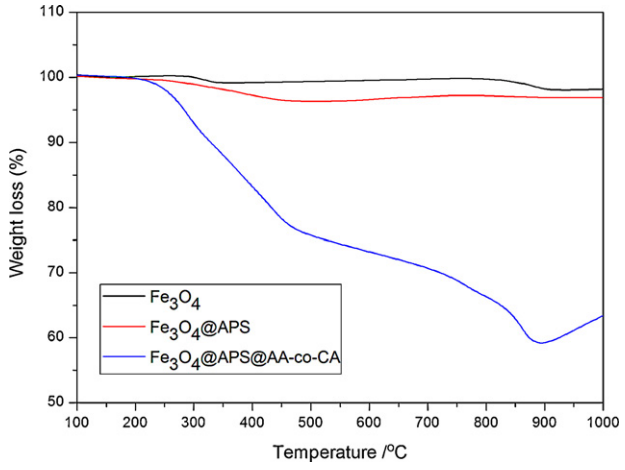

Fig. 3. Thermogravimetric analysis curves for Fe_3O_4, Fe_3O_4@APS and Fe_3O_4@APS@AA-co-CA.

XRD patterns of the 3 MNPs (Supplementary Fig. S2) indicated their cubic spine structures. The reflection peak positions and relative intensities of the MNPs agree well with XRD patterns for MNPs in the literature [25]. The results also indicated that the surface modification of Fe_3O_4 had no effect on the structure of Fe_3O_4 crystal.

3.2. Adsorption properties of the MNPs for metal ions

3.2.1. Effect of pH on adsorption and the mechanism of adsorption

To evaluate the effect of pH, we investigated adsorption of metal ions at pH 1.0–8.0 [9,32]. The initial pH was an important variable for adsorption of the metal ions (Fig. 4). The removal efficiency increased with pH 1.0–4.0 but changed little with pH > 4.0. The observed dependence of adsorption on pH may be attributed to change in the surface of the adsorbents with change in pH, which was consistent with the pH-dependent zeta-potential of Fe_3O_4@APS@AA-co-CA (Supplementary Fig. S3). The pH of zero point charge (pH_{pzc}) was between 3.0 and 4.0. At low pH ($pH < pH_{pzc}$), the surface of the adsorbents presents in carboxyl form and has less adsorption. As the alkalinity of solution increases, the carboxyls turn into carboxylate anions and the adsorption increases gradually until $pH > pH_{pzc}$. After then, carboxyls completely turn into carboxylate anions, with almost no change in adsorption. Considering that the metal ions might precipitate as hydroxide, e.g. Pb^{2+} will first precipitate in pH > 5.5 based on Ksp of metal ions and OH^-, we chose pH 5.5 for further experiments. The probable adsorption mechanism is shown in Fig. 5. The metal ions mainly interacted with the adsorbents by chelation between the ions and the carboxylate anion [33].

3.2.2. Adsorption kinetics

Fig. 6 shows the effects of contact time on the adsorption of the metal ions. The metal ions all rapidly reached equilibrium at 45 min. In fact, 95% of the metal ions were adsorbed at about 30 min. Compared with other reported adsorbents [34], the MNPs we prepared show fast adsorption. The efficiency could be attributed to the larger surface area of MNPs and the higher content of AA-co-CA

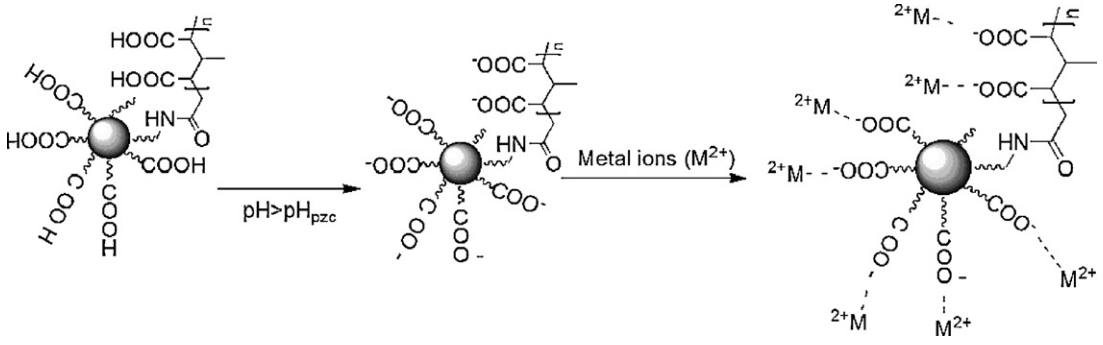

Fig. 5. Schematic representations of possible mechanism for adsorption of metal ions by Fe_3O_4@APS@AA-co-CA.

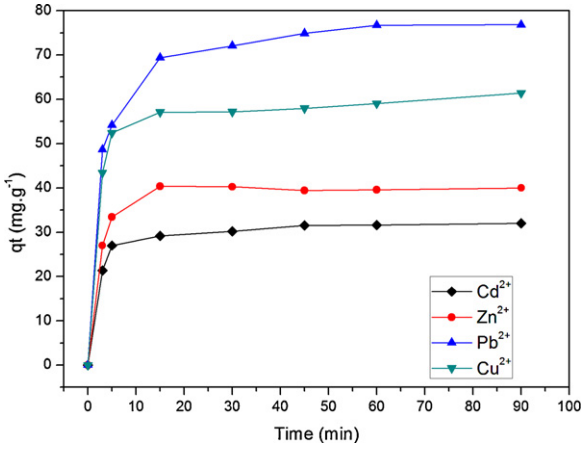

Fig. 6. Effect of time on the adsorption of metal ions; adsorbent: 0.05 g, concentration of metal ions: 100 mg L^{-1}, volume of solution: 50 ml, pH: 5.5, at 298 K.

crosslinked on the Fe_3O_4 MNPs [8]. To ensure the equilibrium, we used shaking for 45 min for all further experiments.

The adsorption kinetics of metal ions with Fe_3O_4@APS@AA-co-CA were investigated by 2 kinetic models: Lagergren pseudo-first-order and pseudo-second-order models, for Eqs. (1) and (2), respectively [13].

Pseudo-first-order model:

$$\ln(q_e - q_t) = \ln\ q_e - k_1 t \tag{1}$$

Pseudo-second-order model:

$$\frac{t}{q_t} = \frac{1}{k_2 q_e^2} + \frac{1}{q_e} t, \tag{2}$$

where q_t (mg g^{-1}) is the adsorption at time t (min); q_e (mg g^{-1}) is the adsorption capacity at adsorption equilibrium; and k_1 (min^{-1}) and k_2 (g mg^{-1} min^{-1}) are the kinetic rate constants for the pseudo-first-order and the pseudo-second-order models, respectively. The kinetic adsorption data were fitted to Eqs. (1) and (2), and the calculated results are in Table 1. The correlation coefficients (R^2) for the pseudo-second-order adsorption model were all higher than for the pseudo-first-order model. Therefore, the adsorption data are well represented by the pseudo-second-order kinetic model. The rate-limiting step of the adsorption was dominated by a chemical adsorption process [32]. This result was expected because the usual exchange processes are more rapid and are controlled mainly by diffusion, whereas those with a chelating exchanger are slower and are controlled by a second-order chemical reaction. In addition, Fe_3O_4@APS@AA-co-CA, which has chelating functional groups on its surface, most probably behaves as a chelating exchanger. Therefore, the complexation chemical reaction is expected in the adsorption processes [35].

We performed time-dependent adsorption kinetics study of Fe_3O_4@APS@AA-co-CA MNPs for metal ions at 3 different temperatures with the pseudo-second-order kinetics Eq. (2). The equation constant k_2 and the equilibrium capacity were both increased with increasing temperature from 298 to 323 K. The phenomenon could be described by the Arrhenius equation defined as the free energy change when one mole of metal ion is transferred from infinity in solution to the surface of the solid [13] (3):

$$\ln k_2 = \ln\ A + \left(\frac{-Ea}{R}\right)\frac{1}{T}, \tag{3}$$

where k_2 is the pseudo-second-order rate constant, A is a temperature-independent factor and Ea is the activation energy of adsorption. The adsorption energy (Ea) for Cd^{2+}, Zn^{2+}, Pb^{2+}, Cu^{2+} obtained from plotting $\ln k_2$ against $1/T$ was 94.7, 71.6, 69.4 and 48.6 kJ mol^{-1}, respectively. The Ea calculated from the Arrhenius equation could be used to estimate the type of adsorption. The positive values of Ea for the metal ions indicate the endothermic process nature of the adsorption process. Free energy change due to chemisorption is more than 8 kJ mol^{-1} [36], which is larger than that due to physisorption. Therefore, the values we obtained indicate that adsorption is likely due to chemisorption.

3.2.3. Adsorption isotherms of Fe_3O_4@APS@AA-co-CA MNPs for the metal ions

The adsorption isotherms could be explained by the Langmuir and Freundlich models, expressed by the Eqs. (4) and (5), respectively.

Table 1
Characteristics of the kinetics models fitted to the experimental results in Fig. 6 for metal ions.

Metal ions	q (mg g^{-1})[a]	1st order			2nd order		
		R^2	k_1	q_e (mg g^{-1})	R^2	k_2	q_e (mg g^{-1})
Cd^{2+}	32.0	0.9152	0.038069	6.971239	0.9982	0.01966	32.5
Zn^{2+}	39.4	0.1833	0.015154	5.957856	0.9957	0.00669	40.2
Pb^{2+}	76.8	0.8534	0.032196	22.08615	0.9968	0.00566	78.8
Cu^{2+}	62.1	0.8030	0.027106	14.98339	0.9979	0.00852	62.4

[a] Experimental values of adsorption capacities.

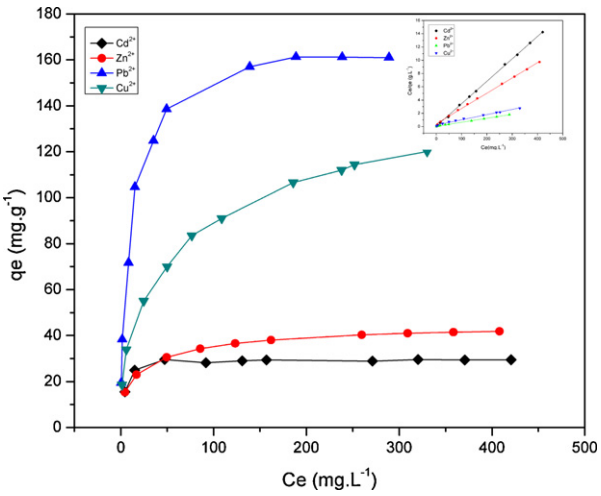

Fig. 7. Equilibrium isotherms of metal ions by Fe_3O_4@APS@AA-co-CA, performed in batch mode; adsorbent: 1.0 g L^{-1}, initial concentration of metal ions, 20–450 mg L^{-1}, temperature: 298 K, pH: 5.5, time: 45 min.

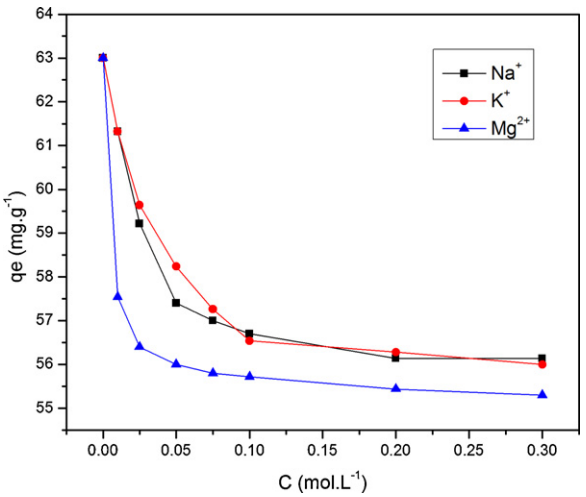

Fig. 8. Effect of the background electrolytes on the adsorption capacity of Fe_3O_4@APS@AA-co-CA for Cu^{2+}.

Langmuir equation:

$$\frac{C_e}{q_e} = \frac{C_e}{q_m} + \frac{1}{K_L q_m}, \quad (4)$$

where q_e is the equilibrium adsorption capacity of ions on the adsorbent (mg g^{-1}); C_e, the equilibrium ions concentration in solution (mg L^{-1}); q_m, the maximum capacity of the adsorbent (mg g^{-1}); and K_L, the Langmuir adsorption constant (L mg^{-1}).

Freundlich equation:

$$q_e = K_F C_e^{1/n}, \quad (5)$$

where equilibrium capacity (q_e) and C_e are defined as above, K_F is the Freundlich constant (L mg^{-1}), and n is the heterogeneity factor [11].

The adsorption isotherm data are in Fig. 7. The q_e of the metal ions was increased with increasing concentrations until reaching equilibrium. The adsorption isotherm data for the metal ions were consistently better with Langmiur than Freundlich isotherms, which were determined by the correlation coefficients (R^2) in Table 2.

The maximum capacity (q_m) for the 4 metal ions calculated by the Langmuir equation differed for the 4 metal ions (Table 2). The q_m for Cu^{2+} reached 1.995 mmol g^{-1}. However, that for Cd^{2+} was just 0.264 mmol g^{-1}. The significant difference should be attributed to the different complex capacity of the carbonyl with the metal ions. The q_m for the metal ions reported for other adsorbents is in Table 3. In general, the MNPs we used had higher adsorption capacity than the reported adsorbents, except for the salicylic acid type of the chelate adsorbent for Cd^{2+} [44]. However, because the density of Fe_3O_4 is larger than polymer, the content of the polymer of Fe_3O_4@APS@AA-co-CA was only 36.7% in weight. Thus, the adsorption capacity of polymer, which plays a dominant role in MNPs, is superior to those adsorbents. Moreover, considering reusability, easy synthesis and separation of MNPs, the Fe_3O_4@APS@AA-co-CA MNPs are better adsorbent than others. In addition, all the Freundlich adsorption intensity variables (n values) were > 2, which supports the favorable adsorption of metal ions with this adsorbent.

3.2.4. Effect of background electrolytes

Heavy metal ion pollutants are often presented together with alkaline/earth metal ions in water systems [38]. The impact of coexisting Na^+, K^+, or Mg^{2+} on the uptake of the Cu^{2+} is in Fig. 8. Although the adsorption capacity of Cu^{2+} with Fe_3O_4@APS@AA-co-CA MNPs significantly decreased with increasing coexisting ions in the region of 0–0.05 mol L^{-1}, the adsorption capacity slightly decreased with ≥0.05 mol L^{-1} coexisting ions; especially, the plateau in the adsorption capacity reached 0.1 mol L^{-1}. The divalent ion, Mg^{2+}, had a more suppressive effect on Cu^{2+} adsorption, likely because of the stronger complexation ability of carbonyl groups with Mg^{2+}. The impact of coexisting electrolytes on the other metal ions was similar to that of Cu^{2+} (Supplementary Figs. S4, S5, S6).

3.2.5. The adsorption isotherms of naked Fe_3O_4 and Fe_3O_4@APS for Cu^{2+}

To confirm the importance of modified polymer, we investigated the adsorption isotherms of naked Fe_3O_4 and Fe_3O_4@APS (Supplementary Fig. S7). The q_m of the naked Fe_3O_4 and Fe_3O_4@APS for Cu^{2+} was 52 and 79 mg g^{-1}, respectively, with higher q_m of Fe_3O_4@APS@AA-co-CA MNPs. Thus, modification of the APS and AA-co-CA on Fe_3O_4 was efficient. Moreover, the adsorption mainly depended on the polymers on the surface of the MNPs.

3.3. Desorption and repeated use

From practical point of view, repeated availability is a crucial feature of an advanced adsorbent [46]. Fig. 4 showed that Fe_3O_4@APS@AA-co-CA MNPs did not significantly adsorb metal ions at pH < 2, which suggested that the adsorbed metal ions could possibly be desorbed in a solution with such pH values [32]. We

Table 2
Langmuir, Freundlich adsorption isotherm constants, correlation coefficients and adsorption capacity.

Metal ions	Langmuir			Freundlich		
	k_L (L mg^{-1})	q_m (mg g^{-1}/mmol g^{-1})	R^2	K_F (mg$^{1-(1/n)}$ $L^{1/n}$ g^{-1})	n	R^2
Cd^{2+}	0.5157	29.6/0.264	0.9995	16.54	9.191	0.5622
Zn^{2+}	0.0554	43.4/0.668	0.9988	12.10	4.577	0.9605
Pb^{2+}	0.1379	166.1/0.802	0.9992	32.93	3.103	0.9940
Cu^{2+}	0.0345	126.9/1.995	0.9886	17.85	2.9303	0.9680

Table 3
Comparison of adsorption capacities of various adsorbents for metal ions.

Type of adsorbent	Adsorption capacities (mg g^{-1})				Reference
	Cd^{2+}	Zn^{2+}	Pb^{2+}	Cu^{2+}	
Magnetic Fe_3O_4 baker's yeast biomass	41.0	-	89.2	-	[37]
Amino-functionalized Fe_3O_4@SiO_2 magnetic nanomaterial	-	-	76.6	30.8	[38]
Sugar beet pulp	24.3	17.7	73.7	21.3	[39]
Copolymer 2-hydroxyethyl methacrylate with monomer methyl methacrylate	-	-	31.5	31.2	[40]
Sporopollenin	6.72	-	93.2	17.2	[41]
Silica-supported dithiocarbamate	40.32	-	70.4	20.36	[42]
Fungal biomass immobilized within a loofa sponge (FBILS)	-	48.9	134.1	98.9	[43]
Salicylic acid type chelate adsorbent	57.1	31.2	86.9	36.9	[44]
Crosslinked chitosan with epichlorohydrin	-	10.2	34.1	35.5	[45]
Fe_3O_4@APS@AA-co-CA MNPs	29.6	43.4	166.1	126.9	This work

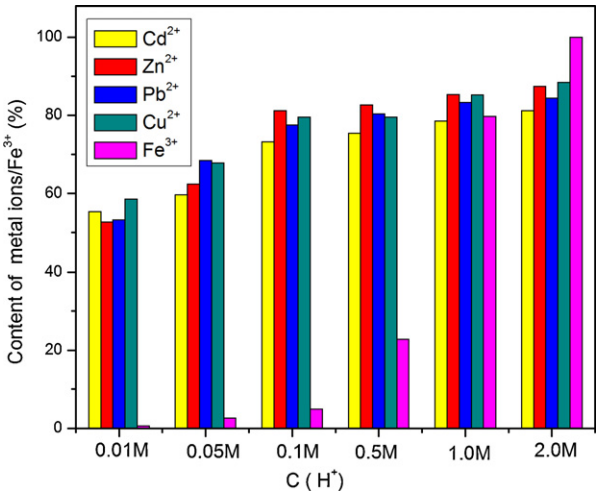

Fig. 9. The contents of the metal ions and Fe^{3+} at different concentrations of H^+.

investigated different concentrations of H^+ to determine the best conditions for reusing MNPs (Fig. 9). The concentration of metal ions increased with increasing H^+ in water but changed little with 0.1 mol L^{-1} H^+. Meanwhile, the adsorbent was corroded by the H^+, which could be seen from the content of the Fe^{3+}. The adsorbent completely disappeared at 2 mol L^{-1} H^+ after 3 h. Considering the desorption efficiency and the reusability cycles of the adsorbents, the initial concentration of 0.1 M H^+ was better than others. The metal ion adsorption capacity of Fe_3O_4@APS@AA-co-CA MNPs remained almost constant for the 4 cycles, which indicates no irreversible sites on the surface of Fe_3O_4@APS@AA-co-CA MNPs for desorption with 0.1 mol L^{-1} H^+, and the reusability of the adsorbents was satisfactory (Fig. 10). Our recyclability studies suggest that this nano-adsorbent can be repeatedly used as an efficient adsorbent in water treatment.

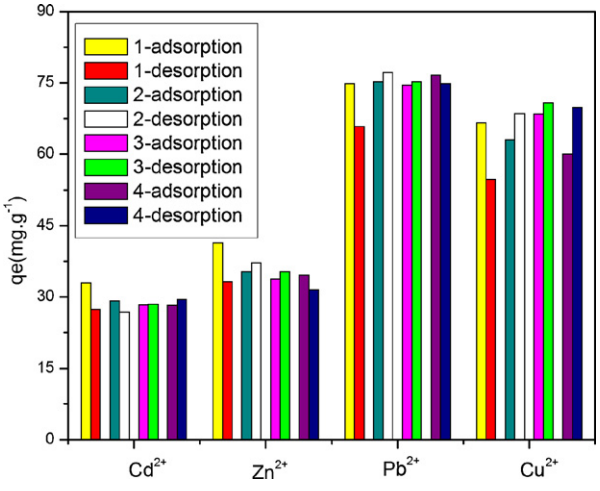

Fig. 10. The performance of Fe_3O_4@APS@AA-co-CA by multiple regeneration cycles.

4. Conclusions

We describe the preparation and characterization of MNPs modified with APS and AA-co-CA (Fe_3O_4@APS@AA-co-CA). Fe_3O_4@APS@AA-co-CA MNPs are excellent for removal of heavy metal ions such as Cd^{2+}, Zn^{2+}, Pb^{2+} and Cu^{2+} from aqueous solution. Furthermore, the MNPs could efficiently remove the metal ions with high maximum adsorption capacity at pH 5.5 and could be used as a reusable adsorbent with convenient conditions.

Acknowledgement

This study was supported by 973 Program (2010CB933504).

Appendix A. Supplementary data

Supplementary data associated with this article can be found, in the online version, at doi:10.1016/j.jhazmat.2011.12.013.

References

[1] A. Wdjtowicz, A. Stokμosa, Removal of heavy metal ions on smectite ion-exchange column, Pol. J. Environ. Stud. 11 (1) (2002) 97–101.
[2] M. Ulewiczi, W. Walkowliak, J. Gega, B. Pospiech, Zinc(II) selective removal from other transition metal ions by solvent extraction and transport through polymer inclusion membranes with D2EHPA, Ars Separatoria Acta 2 (2003) 47–55.
[3] H.C. Yun, R. Prasad, A.K. Guha, K.K. Sirkar'a, Hollow fiber solvent extraction removal of toxic heavy metals from aqueous waste streams, Ind. Eng. Chem. Res. 32 (1993) 1186–1195.
[4] V.C. Taty-Costodes, H. Fauduet, C. Porte, A. Delacroix, Removal of Cd(II) and Pb(II) ions, from aqueous solutions, by adsorption onto sawdust of pinus sylvestris, J. Hazard. Mater. B105 (2003) 121–142.
[5] H. Ozaki, K. Sharmab, W. Saktaywirf, Performance of an ultra-low-pressure reverse osmosis membrane (ULPROM) for separating heavy metal: effects of interference parameters, Desalination 144 (2002) 287–294.
[6] K. Jainaea, K. Sanuwong, J. Nuangjamnong, N. Sukpirom, F. Unob, Extraction and recovery of precious metal ions in wastewater by polystyrene-coated magnetic particles functionalized with 2-(3-(2-aminoethylthio)propylthio)ethanamine, Chem. Eng. J. 160 (2010) 586–593.
[7] Y. Feng, J. Gong, G.M. Zeng, Q.Y. Niu, H.Y. Zhang, C.G. Niu, Adsorption of Cd (II) and Zn (II) from aqueous solutions using magnetic hydroxyapatite nanoparticles as adsorbents, Chem. Eng. J. 162 (2010) 487–494.
[8] Q. Peng, Y. Liu, G. Zeng, W. Xu, Biosorption of copper(II) by immobilizing *Saccharomyces cerevisiae* on the surface of chitosan-coated magnetic nanoparticles from aqueous solution, J. Hazard. Mater. 177 (2010) 676–682.
[9] S.S. Banerjee, D. Chen, Fast removal of copper ions by gum Arabic modified magnetic nano-adsorbent, J. Hazard. Mater. 147 (2007) 792–799.
[10] M.H. Mashhadizadeh, Z. Karami, Solid phase extraction of trace amounts of Ag, Cd, Cu, and Zn in environmental samples using magnetic nanoparticles coated by 3-(trimethoxysilyl)-1-propantiol and modified with 2-amino-5-mercapto-1,3,4-thiadiazole and their determination by ICP-OES, J. Hazard. Mater. 190 (2011) 1023–1029.

[11] K. Shin, J. Hong, J. Jang, Heavy metal ion adsorption behavior in nitrogen-doped magnetic carbon nanoparticles: isotherms and kinetic study, J. Hazard. Mater. 190 (2011) 36–44.
[12] A. Afkhami, M. Saber-Tehrani, H. Bagheri, Simultaneous removal of heavy-metal ions in wastewater samples using nano-alumina modified with 2,4-dinitrophenylhydrazine, J. Hazard. Mater. 181 (2010) 836–844.
[13] Y.M. Hao, M. Chen, Z. Hu, Effective removal of Cu (II) ions from aqueous solution by amino-functionalized magnetic nanoparticles, J. Hazard. Mater. 184 (2010) 392–399.
[14] S. Huang, D. Chen, Rapid removal of heavy metal cations and anions from aqueous solutions by an amino-functionalized magnetic nano-adsorbent, J. Hazard. Mater. 163 (2009) 174–179.
[15] G. Bayramoglu, M. Yakup Arica, Kinetics of mercury ions removal from synthetic aqueous solutions using by novel magnetic p(GMA-MMA-EGDMA) beads, J. Hazard. Mater. 144 (2007) 449–457.
[16] M.H. Liao, D.H. Chen, Fast and efficient adsorption/desorption of protein by a novel magneticnano-adsorbent, Biotechnol. Lett. 24 (2002) 1913–1917.
[17] M.H. Liao, D.H. Chen, Preparation and characterization of a novel magnetic nano-adsorbent, J. Mater. Chem. 12 (2002) 3654–3659.
[18] S.Y. Mak, D.H. Chen, Fast adsorption of methylene blue on polyacrylic acid-bound iron oxide magnetic nanoparticles, Dyes Pigments 61 (2004) 93–98.
[19] Y.C. Chang, D.H. Chen, Preparation and adsorption properties of monodisperse chitosan-bound Fe_3O_4 magnetic nanoparticles for removal of Cu(II) ions, J. Colloid Interface Sci. 283 (2005) 446–451.
[20] S.Y. Mak, D.H. Chen, Binding and sulfonation of poly(acrylic acid) on iron oxide nanoparticles: a novel, magnetic, strong acid cation nano-adsorbent, Macromol. Rapid Commun. 26 (2005) 1567–1571.
[21] S.H. Huang, M.H. Liao, D.H. Chen, Fast and efficient recovery of lipase by polyacrylic acid-coated magnetic nano-adsorbent with high activity retention, Sep. Purif. Technol. 51 (2006) 113–117.
[22] S. Shin, J. Jang, Thiol containing polymer encapsulated magnetic nanoparticles as reusable and efficiently separable adsorbent for heavy metal ions, Chem. Commun. 423 (2007) 0–4232.
[23] M.T. Pham, K.K. Soo, Surface functionalized nano-magnetic particles for wastewater treatment: adsorption and desorption of mercury, J. Nanosci. Nanotechnol. 9 (2009) 905–908.
[24] X. Fu, X. Chen, J. Wang, J. Liu, Fabrication of carboxylic functionalized superparamagnetic mesoporous silica microspheres and their application for removal basic dye pollutants from water, Micropor. Mesopor. Mater. 139 (2011) 8–15.
[25] Y. Zhou, S. Wang, Modification of magnetite nanoparticles via surface-initiated atom transfer radical polymerization (ATRP), Chem. Eng. J. 138 (2008) 578–585.
[26] X. Zhao, J. Wang, F. Wu, T. Wang, Y. Cai, Removal of fluoride from aqueous media by Fe_3O_4@Al $(OH)_3$ magnetic nanoparticles, J. Hazard. Mater. 173 (2010) 102–109.
[27] Y. Zhang, N. Kohler, M. Zhang, Surface modification of superparamagnetic magnetite nanoparticles and their intracellular uptake, Biomaterials 23 (2002) 1553–1561.
[28] S. Bassaid, M. Chaib, A. Bouguelia, M. Trari, Elaboration and characterization of poly (acrylic acid-co-crotonic acid) copolymers: application to extraction of metal cations Pb(II), Cd(II) and Hg(II) by complexation in aqueous media, React. Funct. Polym. 68 (2008) 483–491.
[29] V.A. Kovyazin, A.V. Nikitin, V.M. Kopylov, Reaction of organosilicon amines with dicarboxylic anhydrides, Russ. J. Gen. Chem. 73 (2003) 1072–1076.
[30] I.F. Nata, G.W. Salim, C.K. Lee, Facile preparation of magnetic carbonaceous nanoparticles for Pb^{2+} ions removal, J. Hazard. Mater. 183 (2010) 853–858.
[31] B.R. White, B.T. Stackhouse, J.A. Holcombe, Magnetic γ-Fe_2O_3 nanoparticles coated with poly-L-cysteine for chelation of As(III), Cu(II), Cd(II), Ni(II), Pb(II) and Zn(II), J. Hazard. Mater. 161 (2009) 848–853.
[32] Y.F. Lin, H.W. Chen, P.S. Chien, C.S. Chiou, Application of bifunctional magnetic adsorbent to adsorb metal cations and anionic dyes in aqueous solution, J. Hazard. Mater. 185 (2011) 1124–1130.
[33] S. Singh, K.C. Barick, D. Bahadur, Surface engineered magnetic nanoparticles for removal of toxic metal ions and bacterial pathogens, J. Hazard. Mater. 192 (2011) 1539–1547.
[34] Q. Peng, Y. Liu, G. Zeng, Biosorption of copper(II) by immobilizing *Saccharomyces cerevisiae* on the surface of chitosan-coated magnetic nanoparticles from aqueous solution, J. Hazard. Mater. 177 (2010) 676–682.
[35] Y.T. Zhou, B.W. Christopher, H.L. Nie, Adsorption mechanism of Cu^{2+} from aqueous solution by chitosan-coated magnetic nanoparticles modified with α-ketoglutaric acid, Colloid Surf. B 74 (2009) 244–252.
[36] L. Zhou, J. Jin, Z. Liu, X. Liang, C. Shang, Adsorption of acid dyes from aqueous solutions by the ethylenediamine-modified magnetic chitosan nanoparticles, J. Hazard. Mater. 185 (2011) 1045–1052.
[37] M. Xu, Y. Zhang, Z. Zhang, Y. Shen, Study on the adsorption of Ca^{2+}, Cd^{2+} and Pb^{2+} by magnetic Fe_3O_4 yeast treated with EDTA dianhydride, Chem. Eng. J. 168 (2011) 737–745.
[38] J. Wang, S. Zheng, Y. Shao, J. Liu, Amino-functionalized Fe_3O_4@SiO_2 core–shell magnetic nanomaterial as a novel adsorbent for aqueous heavy metals removal, J. Colloid Interface Sci. 349 (2010) 293–299.
[39] Z. Reddad, C. Gerente, Y. Andres, Adsorption of several metal ions onto a low-cost biosorbent: kinetic and equilibrium studies, Environ. Sci. Technol. 36 (2002) 2067–2073.
[40] O. Moradi, M. Aghaie, K. Zarea, M. Monajjemi, H. Aghaiea, The study of adsorption characteristics Cu^{2+} and Pb^{2+} ions onto PHEMA and P(MMA-HEMA) surfaces from aqueous single solution, J. Hazard. Mater. 170 (2009) 673–679.
[41] N. ünlü, M. Ersoz, Removal of heavy metal ions by using dithiocarbamated-sporopollenin, Sep. Purif. Technol. 52 (2007) 461–469.
[42] L. Bai, H. Hu, W. Fu, Synthesis of a novel silica-supported dithiocarbamate adsorbent and its properties for the removal of heavy metal ions, J. Hazard. Mater. 195 (2011) 261–275.
[43] M. Iqbal, R.G.J. Edyvean, Biosorption of lead, copper and zinc ions on loofa sponge immobilized biomass of *Phanerochaete chrysosporium*, Miner. Eng. 17 (2004) 217–223.
[44] F. An, B. Gao, X. Dai, Efficient removal of heavy metal ions from aqueous solution using salicylic acid type chelate adsorbent, J. Hazard. Mater. 192 (2011) 956–962.
[45] A.H. Chen, S.C. Liu, C.Y. Chen, Comparative adsorption of Cu(II), Zn(II), and Pb(II) ions in aqueous solution on the crosslinked chitosan with epichlorohydrin, J. Hazard. Mater. 154 (2008) 184–191.
[46] A.Z.M. Badruddoza, A.S.H. Tay, P.Y. Tan, K. Hidajat, M.S. Uddin, Carboxymethyl-β-cyclodextrin conjugated magnetic nanoparticles as nano-adsorbents for removal of copper ions: synthesis and adsorption studies, J. Hazard. Mater. 185 (2011) 1177–1186.